



Investigation of mass transport phenomena in an upflow cold-wall CVD reactor by gas phase Raman spectroscopy and modeling

Jang Y. Hwang^a, Chinho Park^b, Min Huang^a, Tim Anderson^{a,*}

^aDepartment of Chemical Engineering, University of Florida, 300 Weil Hall, Gainesville, FL 32611, USA

^bYeungnam University, School of Chemical Engineering and Technology, Gyeongsan 712-749, Republic of Korea

Received 15 February 2005; accepted 16 February 2005

Available online 9 April 2005

Communicated by J.J. Derby

Abstract

Steady and transient mass transport phenomena within an inverted, stagnation-flow, cold-wall CVD reactor were investigated by observing the concentration of a tracer species (CH₄) with in situ Raman spectroscopy. The transient studies revealed that the use of matched reactor inlet velocities is crucial to minimize recirculating flow patterns and that the magnitude of the gas velocity is also important in gas switching. In the steady-state studies, it was observed that the existence of a sufficiently large density gradient in the reactor initiates natural convection and under some conditions introduces a flow instability and thus three-dimensional (3-D) flows. The onset of instability was characterized by solutal density difference, gas velocity, and distance traveled by the gas. A steady-state, 2-D axisymmetric reactor model validated with experimental data was used to analyze the measured tracer concentration profiles.

© 2005 Published by Elsevier B.V.

PACS: 52.75.R; 47.32; 82.80.C; 47.11

Keywords: A1. In situ Raman spectroscopy; A1. Mass transfer; A1. Stagnation-point-flow reactor; A1. Two-dimensional axisymmetric reactor model

1. Introduction

It is possible to grow a variety of thin film materials by chemical vapor deposition (CVD) using a wide range of reactor designs [1–3]. For a given design, the thickness and composition uniformity of deposited films and the interface

*Corresponding author. Tel.: +1 352 392 0946; fax: +1 352 392 9513.

E-mail address: tim@ufl.edu (T. Anderson).

abruptness of layered structures are largely influenced by the gas dynamics including mass transport in the reactor. To achieve desirable mass transport behavior, it is important to establish a stable, vortex-free flow field in the reactor. Recirculating flow patterns can cause varied growth rate, increased impurity incorporation, and graded heterojunctions [4,5]. Furthermore, the growth efficiency can be significantly reduced by the presence of parasitic gas phase reactions in the recirculating flow cells [6,7]. The method of gas switching can also affect the layer abruptness if dead space is present in the gas-handling manifold, or if the transient response time becomes too long due to a pressure imbalance in the switching manifold [8,9]. Although there have been many studies of transport phenomena in CVD reactors, most have been limited to modeling studies solving the momentum and energy equations of change, with very little effort devoted to measurement of mass transport phenomena.

The flow pattern in a CVD reactor is influenced by several factors including the reactor geometry, heat transfer characteristics, and the flow boundary conditions. The influence of buoyancy forces due to thermal effects has been extensively studied in CVD reactors [10–12]. A large thermal gradient not aligned with the direction of the gravity vector can produce recirculating flow patterns in the reactor and cause adverse effects on the film quality [10,13–16]. It is also reported that the buoyancy caused by temperature gradients can break the condition of axisymmetry to trigger flow instability and give three-dimensional (3-D) flows [10,11]. Recirculation or unstable flow patterns should be eliminated or at least minimized for satisfactory process control and reproducibility. With respect to recirculation flow, an inverted reactor geometry in which cold gas flows up toward the heated substrate has certain advantages because the buoyancy tends to stabilize the flow.

In addition to thermal gradients, density gradients from concentration variations in CVD reactors are not avoidable even at room temperature and therefore these buoyancy-driven flow phenomena should be considered when reactors are designed, scaled, and/or optimized. Solutal convection in a down flow reactor was predicted

by numerical simulations [17] and observed by a flow visualization technique [9]. The gas velocity, inlet-to-susceptor distance, and density variation are important parameters for characterizing the observed solutal convection. Switching metal-organic sources will impose density variations in the CVD reactor and therefore should be properly handled when growing layered structures. Inlet gas compositions and velocities should be carefully selected, since they can also affect flow patterns in the reactor. Therefore, understanding gas dynamics in CVD processes including mass transport phenomena and their effects on the reactor flow dynamics is as important as understanding the energy transport.

In this study, mass transport was studied in an inverted, stagnation-flow CVD reactor by profiling a tracer species using *in situ* Raman spectroscopy. The transient response to reactant switching and the steady-state transport behavior as a function of inlet velocity and reactor aspect ratio were experimentally investigated. The studies were performed at room temperature to focus on mass transfer effects.

2. Experimental and modeling details

A custom designed, up flow, cold-wall CVD reactor was used in this study that incorporated an axisymmetry reactor design to simplify the modeling work. Gases were introduced through three concentric inlets at the bottom of the reactor and flowed toward a susceptor directly facing the inlets at an adjustable distance. This reactor was designed to directly interface with a Raman spectrometer to study gas phase CVD reactions, and the detailed reactor design is described in detail elsewhere [16]. It is noted that the gas inlet configuration in this study was modified from a 2-inlet configuration (center and sweep flows) used in the previous studies [16,18] to a 3-inlet design (center, annulus, and sweep flows, starting from the centerline) as illustrated in Fig. 1. The annulus inlet was partially filled with glass beads, while the center inlet was not packed. The unpacked height in the annulus was set at 65 mm. The sweep inlet

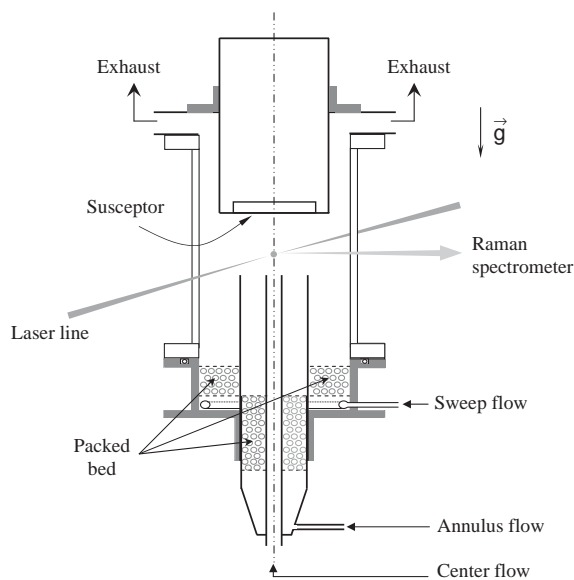


Fig. 1. Inlet configuration of the upflow CVD reactor.

was also partially filled with glass beads to help provide a uniform gas distribution at the inlet.

As a probing tool, a Ramanor U-1000 Raman spectrometer from Jobin–Yvon was coupled with the reactor, and a 488 nm line of an Ar-ion laser was used as the light source. The laser line was focused into a spatial point inside the reactor with a lens and the scattered Raman signals from the point as collected at a right angle to the incident laser line. Raman spectroscopy is capable of providing both chemical species information and gas phase temperature with good spatial resolution, and therefore is a suitable technique to gather in situ information on mass transport in a non-invasive fashion [19,20].

To evaluate the transient mass transport response of the system to reactant switching, a pulsed injection of a probe gas, 10% methane in hydrogen, was introduced through the center inlet to the reactor and the concentration of methane was measured by Raman scattering as a function of time. The center inlet tube was lowered in this case to the bottom so that the combined center and annulus inlets formed a single inlet separated from the sweeping flow. Before the pulse was introduced

to the combined center/annulus inlet, a carrier gas, hydrogen, was constantly flowing in the sweep and center/annulus inlets. During the switching process, constant velocities at the inlets were maintained at specified values by using make-up carrier gas streams. The pulse duration was 20 s and the Raman intensity of the C–H stretching vibration of methane at 2917 cm^{-1} was monitored with time at 12 mm below the susceptor surface on the centerline of the reactor (see Fig. 1). The transient response was measured for different values of inlet gas velocities, including matched and unmatched sets.

The mass transport phenomena at steady state were investigated by introducing a stream of methane diluted with nitrogen through the annulus inlet and pure nitrogen through the center and sweep inlets. The inlet methane concentration was varied from 1.9% to 14.5%, and the methane concentration in the reactor was obtained from the Raman scattering signals detected along the centerline of the reactor. The relative Raman cross-section of the C–H stretching vibration of methane with respect to the Q-branch of nitrogen at 2331 cm^{-1} was estimated to be 8.34 from the measurements of this study and it agreed well with the reported range [21].

Previously, a heat transport model of the current reactor was built and thermal effects on the gas dynamics have been reported and validated with experimental data [16]. Based on the previous gas dynamics study, a 2-D axisymmetric reactor model including mass transport was developed to analyze steady-state mass transport in the reactor. The Galerkin finite element method was used for numerical calculations and the pressure term in the equation of change for momentum was eliminated by using the penalty function formulation [22]. In the species balance equations, diffusive and convective mass transport modes were incorporated [23]. The numbers of elements and nodes used in calculations were 6431 and 6608, respectively. A specific value for the inlet methane concentration was given at the bottom of the annulus, while zero concentration was specified at the other two inlets and a no penetration condition was set at the walls. A detailed description of the solution method was previously given [16].

3. Results and discussion

3.1. Transient mass transport studies

Achieving rapid and abrupt reactant switching requires low residence times and avoidance of closed streamline flows. As an example, the shearing action of two parallel flows at different velocity can easily produce flow recirculation patterns. The effect of not matching the inlet gas velocities is shown by the measured response illustrated in Fig. 2. In the comparison, two sets of velocity setting were used: the unmatched combination of 3.0 and 0.75 cm/s for the center and sweep inlets (Fig. 2a), respectively, and the other of 3.0 cm/s for both inlets (Fig. 2b). Both recorded Raman scattering responses include identical time lags of ~ 12 s as a result of the residence time from the run/vent switching manifold to the probe position inside the reactor. The rate at which the signal intensity increases upon the appearance of methane is high but finite, with ~ 10 s required to reach a maximum signal strength. This finite rate is due to axial, and to a lesser extent transverse, dispersion of the methane pulse. The signal from the 20 s pulse then remains relatively constant for about 10 s before decreasing. It is finally noted that the signal contains

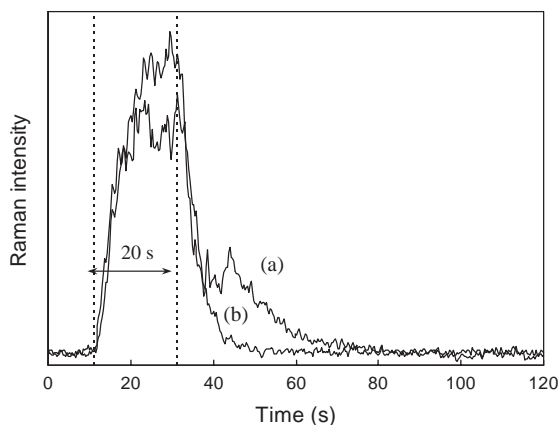


Fig. 2. Transient response of hydrogen-diluted methane pulse for (a) unmatched and (b) matched inlet velocities at 25 °C. For the unmatched case, 3.0 and 0.75 cm/s were set for the center and the sweep, respectively. For the matched case, 3.0 cm/s was set for both inlets. The pulse was introduced for initial 20 s.

significant fluctuations in time that are greater than the estimated signal noise as evidenced by the baseline signal intensity. This suggests that real variations in CH₄ concentration are present in the small sampling volume on a time scale much shorter than the pulse time. These fluctuations in concentration during gas switching could significantly affect on the growth process.

A trapezoidal pulse with a shoulder peak was observed for the unmatched case, while a single trapezoidal pulse was observed when the inlet velocities were matched. The presence of the shoulder peak indicates that there was at least one recirculation pattern in the reactor, which acts as a reservoir of the source material, methane. As observed, gas-switching performance is poor if a recirculation pattern is present, taking more than twice the time to decay in this example. As expected, the matched velocity combination is preferred to establish a non-circulating flow pattern in the reactor.

In gas switching, the magnitude of the gas velocity itself can also be an important factor. To study this effect, three separate matched inlet velocity values were tested at room temperature: 0.75, 1.5, and 3.0 cm/s. A clear trapezoidal pulse was recorded in the 3.0 cm/s case, while the response became broader for the lower velocities and small shoulder peaks were evident (Fig. 3). It

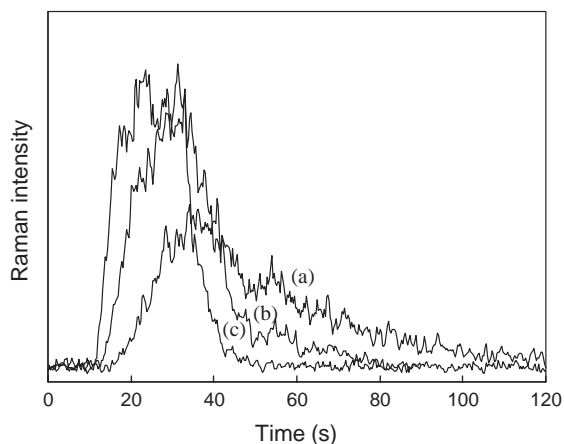


Fig. 3. Transient response of hydrogen-diluted methane pulse for matched velocity cases at 25 °C. The velocities were (a) 0.75, (b) 1.5, and (c) 3.0 cm/s, respectively.

is also seen that a lower velocity increases the residence time to permit an increased extent of dispersion. The shoulder peaks seen in Fig. 3a and b again indicate the presence of weak steady recirculation patterns in the reactor. Recirculation flow patterns within single gas inlet, down flow reactors have been studied experimentally [9] and numerically [24]. It is well known that thermal gradients in the reactor can produce natural convection [10,11,16], and that the natural convection can be effectively suppressed in several ways including the use of an inverted reactor geometry and high gas velocity [12,16,25]. It was also reported that the buoyancy due to thermal gradients could break the intended flow symmetry and lead to a flow instability, and the characteristic length of the 3-D flow was the reactor diameter [11]. In many CVD processes, however, the molecular weight differences between the reactant and carrier gas species can also produce significant density variations to drive natural convection. Since a 10% CH₄/H₂ mixture was flowing in the center inlet line and pure hydrogen in the sweep line, a large transverse density gradient exists and presumably is the cause of the observed recirculation flow under isothermal conditions (room temperature).

3.2. Steady-state mass transport studies

A series of room temperature, steady-state experiments were performed to better understand the influence of the flow conditions and reactor geometry on mass transport. In the first set of experiments the mass transport of a tracer species introduced in the annulus region was evaluated. In these experiments, a methane/nitrogen mixture of variable composition was introduced at the annulus inlet, while pure nitrogen was introduced at the center and sweep inlets. The steady-state methane concentration profile that developed along the centerline was then measured. Three values of the inlet velocity were studied (2.5, 3.5, and 4.5 cm/s), while maintaining a matched velocity condition for all three inlets. The methane concentration at the annulus inlet was also varied (1.91%, 1.36%, and 1.06% for the 2.5, 3.5, and 4.5 cm/s inlet velocity conditions, respectively).

Measured concentration profiles for the three cases are presented in Fig. 4. As expected the methane concentration along the centerline increases as the distance from the inlet increases as a result of transverse mass transport from the annulus region, presumably by diffusion. As the velocity increases, the residence time decreases and the total transverse mass transport decreases accordingly. The vertical broken line in the figure denotes the position of the inlet tips and the error bars represent 99% confidence interval of each measured methane concentration. The solid lines in Fig. 4 convey simulation results using the 2-D mass transport model, which reproduce the corresponding experimental data well. Although the simulation results fall within the confidence limits, the experimental data in this figure show a systematic positive deviation near the inlet tips, which becomes larger at higher inlet gas velocity. It is likely that the finite thickness of the inlet tubes disrupted the streamlines and promoted transverse mixing. Considering that no adjustable parameters were used in the model other than the input experimental conditions, the model appears to capture the primary mass transport mechanisms.

The validated model was then used to calculate steady-state concentration profiles in the reactor

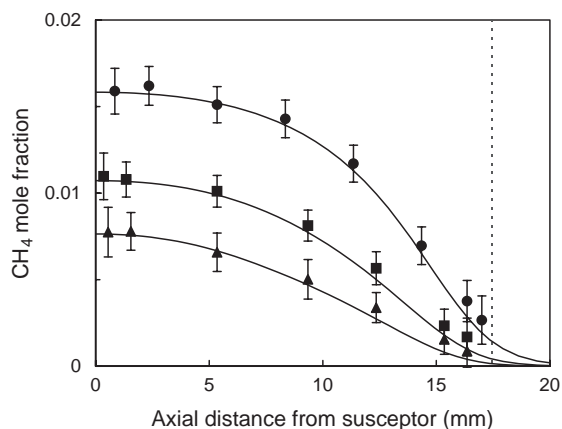


Fig. 4. Methane concentration profiles at 24°C along the centerline for three inlet velocity values: 2.5 (●), 3.5 (■), and 4.5 (▲) cm/s. Solid lines are from simulations. The inlet methane concentrations are 1.91%, 1.36%, and 1.06% for 2.5, 3.5, and 4.5 cm/s, respectively. The vertical dashed line denotes the inlet position.

for various operating conditions to select interesting experimental conditions. As an example, Fig. 5 shows calculated radial concentration profiles at three axial positions (1, 8 and 14 mm below the susceptor) for the 2.5 cm/s matched inlet velocity case. In this calculation a 1.91% methane in nitrogen mixture was introduced at the annulus inlet, while pure N₂ was delivered at both the center and sweep inlets. The methane confined to the annulus at the inlet position then disperses towards both the centerline of the reactor and wall. The calculated radial concentration profiles seem reasonable when the flow characteristics of a stagnation-flow reactor with diffusive mass transport are taken into account. This figure reveals that the CH₄ probe gas is effectively isolated from the reactor wall at $r = 35$ mm. Such species confinement to the gas phase is often desired to avoid complexities caused by reactions at the wall, for example, in the study of gas phase decomposition of metalorganic precursors. The wide range of reported values of the activation energy for trimethylaluminum (TMAI) pyrolysis (38 [26] to 158.6 kJ/mol [27]) are likely related to complications from uncontrolled surface reactions.

In addition to adjusting the inlet velocity and gas composition, the position of the inlet relative to the susceptor is a common design variable.

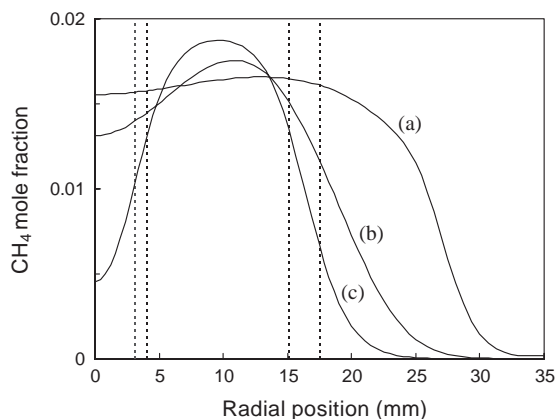


Fig. 5. Radial methane concentration profiles at three different axial positions, (a) 1, (b) 8, and (c) 14 mm below the susceptor. The inlet velocities were matched at 2.5 cm/s and the annulus CH₄ concentration was 1.9% in N₂. The vertical broken lines represent the inlet wall positions at 17.5 mm below the susceptor.

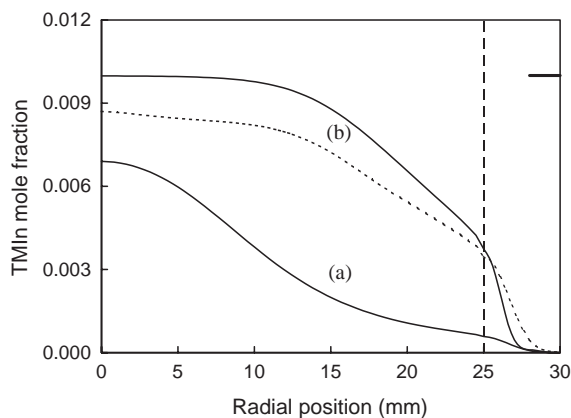


Fig. 6. Calculated radial concentration profiles of TMIn for aspect ratios of 1.0 (a) and 0.5 (b). The inlet gas velocities were matched at 3.0 cm/s and the TMIn concentration was 1.0% (marked by the horizontal bar) at the center inlet. The radius of the susceptor is 25 mm (vertical dashed line) and the reactor wall is positioned at 31 mm.

Fig. 6 shows the calculated radial concentration profile of trimethylindium (TMIn) at aspect ratios 1 and 0.5 for 3.0 cm/s matched inlet velocities (the heater temperature was 900 °C, but no reactions were considered). The aspect ratio is defined as the ratio of the separation distance between the substrate and the inlet to the inlet diameter. In this calculation, a 1.0% TMIn in N₂ mixture was introduced to the reactor at the combined center-annulus inlet, where the center tube in Fig. 1 was lowered to the bottom position. It is desirable that the radial concentration profiles of reactants near the substrate be uniform to deposit good-quality films. As shown in Fig. 6, the radial concentration profiles near the substrate depend significantly on the value of the aspect ratio. For a given velocity, a smaller aspect ratio gives less residence time and thus less radial transport and better uniformity at the substrate. The dashed concentration profile in this figure was calculated with rotation of the substrate at 60 rpm. As expected, rotating the substrate helps establish a flatter concentration profile near the substrate.

In applications of the reactor to measure transport and gas phase kinetics, the optimal conditions to estimate mass diffusivity are different from those used to study homogenous reactions. On one hand, if the reactor is being used to

investigate pure mass transport behavior of chemical species and extract their transport properties (e.g., gas diffusivity), it is better to establish an axial concentration profile showing large gradients. On the other hand, to study reactions and estimate reaction rate constants from the measured profiles, it is better to have a centerline concentration that shows little variation, since observed variations in centerline concentration are then primarily determined by the extents of reactions.

Large concentration gradients are often present in reactors; for example when sweeping flows of carrier gas are used to prevent sidewall reactions or reactants are introduced separately to minimize premature gas phase reactions. Secondary flow driven by solutal variations can be significant and reduce the reactor performance. To study solutal effects, experiments and simulations were performed in which large methane concentration gradients in nitrogen were introduced. As an example, Fig. 7 shows methane concentration profiles calculated and measured along the centerline when a CH₄/N₂ mixture was injected in the annulus at three different methane concentrations (1.9%, 5.0%, and 7.5% CH₄) for a matched inlet velocity of 2.5 cm/s and aspect ratio = 0.5. The results in Fig. 7 show that the validated model was able to reproduce the experimental data for the

two lower CH₄ concentration cases but not for the 7.5% CH₄ case. This discrepancy was not produced by the presence of stable recirculation flow patterns in the reactor. In the 5.0% case, for example, the model predicts recirculation patterns (not presented here), but still reproduced the experimental concentration profile well. These observations imply that the flow regimes were considerably changed for the 7.5% case and the model was not capable of describing flows in the new regime.

To better understand the nature of this new regime, axial methane concentrations were measured at two radial positions, $r = 0$ and 10 mm, when introducing 10% CH₄ in nitrogen through the annulus inlet and pure N₂ through the center and sweep inlets with the inlet matched gas velocity of 1.5 cm/s. It was anticipated that these experimental conditions push the flow pattern into the new regime. The experimental results are represented in Fig. 8. The concentrations denoted by open circles were axially measured along the centerline (at $r = 0$ mm) and those denoted by filled circles were at $r = 10$ mm, which is close to the middle of the annulus region. The simulation results are presented as the broken ($r = 0$) and solid ($r = 10$ mm) lines in this figure.

The considerable differences between experimental and calculated concentrations apparently

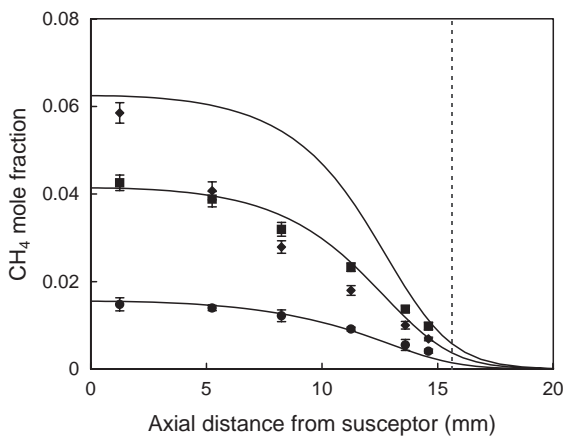


Fig. 7. Axial concentration profiles of methane with three inlet concentrations at 23.3 °C: (a) 1.91% (●); (b) 5.0% (■); (c) 7.5% (◆). Gas velocities are set at 2.5 cm/s for all cases. The vertical dashed line denotes the inlet position.

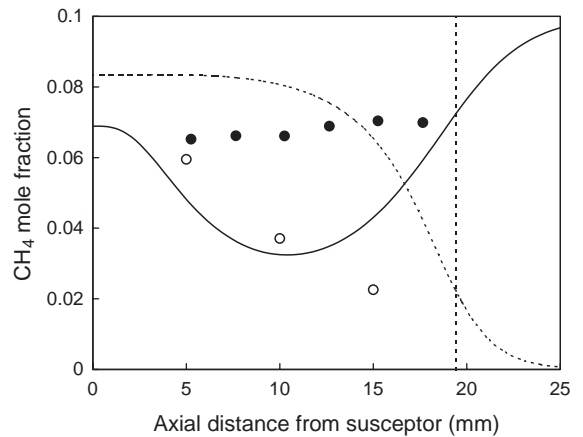


Fig. 8. Axial concentration profiles of methane at $r = 0$ mm (○, ---) and $r = 10$ mm (●, —) at 24 °C. The inlet concentration was 10% and velocity was set at 1.5 cm/s. The vertical dashed line denotes the inlet position.

denote that the experimental methane transport toward the centerline of the reactor was efficiently restrained and methane remains around the initial radial position while flowing axially. As the calculations with the validated 2-D mass transport model predicted (Fig. 8), the flow strength in this case is not sufficiently strong to suppress observable mass transport (diffusion) as efficiently as shown in the experimental observations. Furthermore, if a flow instability occurs only in the center and annulus flow regions, the concentrations along the centerline will be higher than the calculations with the model due to effective gas mixing in the center and annulus flow regions. For the same reasons, mixing of methane and nitrogen would be enhanced even if the flow pattern was time-dependent. Therefore, it is considered that the flow in the reactor was no longer 2-D and fresh N_2 was supplied from the sweep (pure N_2) flow.

Using the validated 2-D mass transport model, streamlines and contour lines in the reactor were calculated for 10% CH_4/N_2 with and without gravity at a gas velocity of 1.5 cm/s to determine the effects of buoyancy on mass and momentum transport. Comparing Fig. 9a and b, there is a strong buoyancy (i.e., with gravity turned on) driving force that pushes the sweep flow toward the centerline of the reactor. As long as the driving force is symmetric along the z -axis, the flow will remain 2-D, i.e., axisymmetric, and consistent with the 2-D mass transport model. The experimental observations (Figs. 7 and 8), however, suggest that the balance can be disrupted when the driving force is sufficiently large to produce a 3-D flow pattern by breaking the symmetry in the flow pattern. Onset of a 3-D flow from a stable axisymmetric flow due to thermally driven buoyancy was predicted in a downward stagnation-flow reactor [11]. It was shown that the 3-D flow produced an axial temperature profile that could not be predicted with a 2-D axisymmetric flow model. In the current case, a large solutal density gradient apparently triggers a flow instability that alters the flow regime.

The steady-state experimental results presented thus far included a 65 mm region before exiting the annulus inlet without packing. This free space was put in the annulus to establish a fully developed

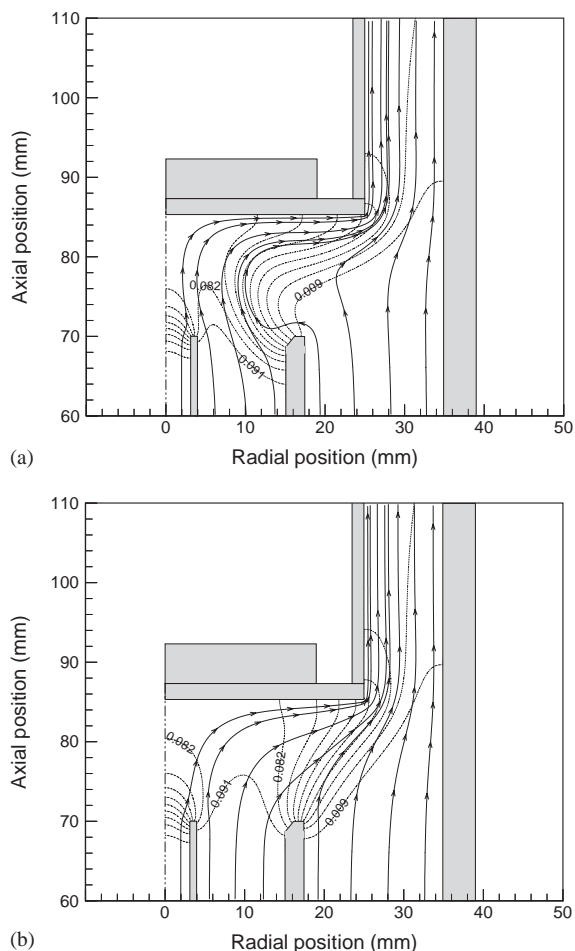


Fig. 9. Streamlines and concentration contours in the reactor when 10% CH_4/N_2 is introduced through the annulus inlet with (a) and without (b) gravity. The gas velocity is 1.5 cm/s for both cases.

flow boundary condition to simplify the simulations. The free space, however, should promote the occurrence of instability by increasing the characteristic length if the distance traveled by the gas is an important length scale. To test this hypothesis, the annulus was filled with glass beads to leave only 6 mm of free space in the annulus and the other inlets remained the same as before. With this modified inlet configuration, two concentration cases, 10% and 14.5%, were examined at a single gas velocity (2.5 cm/s). The CH_4 concentration was probed along the centerline, and the experimental and calculated results are compared

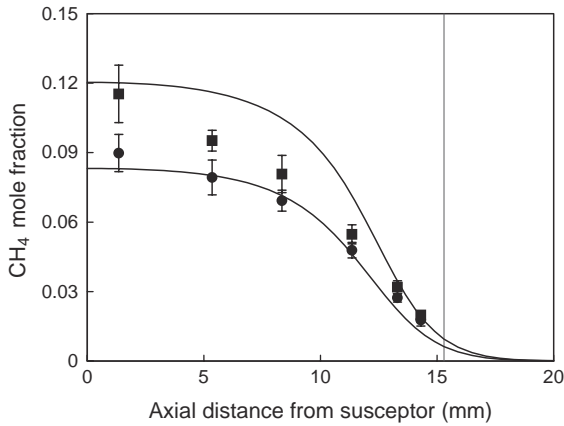


Fig. 10. Axial concentration profiles of methane with reduced free space at the annulus at 2.5 cm/s and 23 °C: 10% (●) and 14.5% (■). The vertical dashed line denotes the inlet position.

in Fig. 10. The aforementioned results in Fig. 7 showed that the model was not able to reproduce experimental data when the methane concentration was higher than 7.5% at 2.5 cm/s. The 2-D model, however, reproduced the experimental results reasonably well even for the higher concentration (10%) when the length of the free space in the annulus was reduced. This suggests that the free space in the annulus, through which the diluted CH₄/N₂ mixture travels, affects the onset of the flow instability and that the distance beyond the packing could be an important characteristic length for the onset of an instability. An even higher methane concentration (14.5%), however, caused experimental measurements to significantly deviate from the calculated concentration profile again (Fig. 10).

The observed influence of the annulus packing on the driving force motivated recalculation of the 10% methane case shown in Fig. 9a, but with a fully packed annulus. The results of calculation, shown in Fig. 11, show that the methane concentration is more uniform, i.e., the area under the concentration contour of 0.082 increases, by filling the annulus channel. At the same time, the degree of pushing by the sweep flow becomes weaker and therefore flow in the reactor tends to be stabilized.

Theses observations and calculation results suggest that density differences produced by

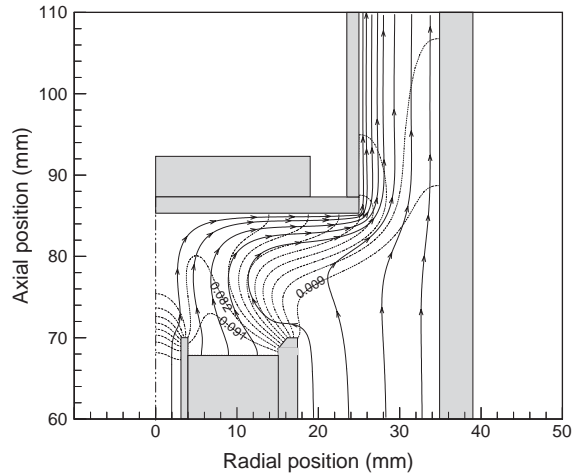


Fig. 11. Effects of filling the annulus channel on streamlines and concentration contours. The initial concentration is 10%. The reference state is shown in Fig. 9a.

concentration variations are important. The dimensionless group Gr/Re^2 represents the relative strength of the buoyancy forces to inertial forces and for this set of experiments is given by

$$\frac{Gr}{Re^2} = \frac{gL\Delta\rho}{V^2\rho} \approx \frac{gL}{V^2} \left(1 - \frac{M_{CH_4}}{M_{N_2}}\right) x_{CH_4}, \quad (1)$$

where the characteristic length scale, gravity, velocity scale, density, molecular weight, and mole fraction are represented by L , g , V , ρ , M , and x , respectively. The second part of the equation includes the assumption of an ideal gas. The effects of the mass average inlet gas velocity (V), concentration (x_{CH_4}), and distance between the susceptor and top of the packing in the inlet (L) on the instability can be explained with this dimensionless group. The values of this dimensionless group are, respectively, 14 and 21 for the 10% and 14.5% CH₄ cases in Fig. 10. The critical values of the dimensionless group for transition from 2-D to 3-D flow are not known. It is, however, considered that the relative strength of the buoyancy forces to inertial forces has different dependence on the characterizing terms, depending on the reactor geometry and specific boundary conditions as reported in the thermal buoyancy case [10]. For example, it was reported [28] that natural convection started to influence flow patterns in a rotating

disk system when a similar term to the dimensionless group was 0.025, which is smaller than 1.

4. Conclusions

Concentration profiles of CH₄ in a carrier gas, hydrogen or nitrogen, in an inverted, stagnation-flow, cold-wall reactor were measured by in situ Raman spectroscopy and used to study gas-switching and steady-state mass transport. Transient gas-switching experiments showed that using high and identical values of the gas velocity at each inlet were critical in preventing the appearance of recirculation flow patterns in the reactor. A steady-state, 2-D mass transport model was developed and validated, and was used to predict the effect of gas velocity, reactant concentration, and aspect ratio on the mass transport. It was found that solutal density variations produce natural convection and can even trigger flow instability in the reactor and give a 3-D flow pattern. In typical CVD reactors, the density distribution produced by concentration variations can be a significant driving force for natural convection. Therefore, buoyancy driven by solutal density variations should be carefully considered when CVD processes are designed, scaled, and optimized. The distance between the susceptor and inlets, concentration difference, and gas velocity were important for the onset of the new flow regime.

Acknowledgments

Authors would like to thank Mr. J. Hinnant and Mr. D. Vince for their kind support during the experiments.

References

- [1] O. Ambacher, *J. Phys. D* 31 (1998) 2653.
- [2] J.P. Hirtz, M. Razeghi, M. Bonnet, J.P. Duchemin, in: T.P. Pearsall (Ed.), *GaInAsP Alloy Semiconductors*, Wiley, New York, 1982 (Chapter 3).
- [3] W.L. Holstein, *Prog. Crystal Growth Charact.* 24 (1992) 111.
- [4] K.F. Jensen, *J. Crystal Growth* 98 (1989) 148.
- [5] Y. Monteil, R. Favre, A. Bekkaoui, P. Raffin, J. Bouix, J. Marcillat, P. Dutto, *J. Crystal Growth* 93 (1988) 270.
- [6] C.H. Chen, H. Liu, D. Steigerwald, W. Imler, C.P. Kuo, M. Ludowise, S. Lester, J. Amano, *J. Electron. Mater.* 25 (1996) 1004.
- [7] C. Theodoropoulos, T.J. Mountziaris, H.K. Moffat, J. Han, *J. Crystal Growth* 217 (2000) 65.
- [8] F. Agahi, C.R. Lutz, K.M. Lau, *J. Crystal Growth* 139 (1994) 344.
- [9] S.C. Palmateer, S.H. Groves, C.A. Wang, D.W. Weyburne, R.A. Brown, *J. Crystal Growth* 83 (1987) 202.
- [10] D.I. Fotiadis, S. Kieda, K.F. Jensen, *J. Crystal Growth* 102 (1990) 441.
- [11] H.V. Santen, C.R. Kleijn, H.E.A. V.D. Akker, J. *Crysal Growth* 212 (2000) 311.
- [12] G. Wahl, *Thin Solid Films* 40 (1977) 13.
- [13] L.J. Giling, *J. Electrochem. Soc.* 129 (1982) 634.
- [14] K.F. Jensen, D.I. Fotiadis, T.J. Mountziaris, *J. Crystal Growth* 1 (1991) 107.
- [15] S. Patniak, R.A. Brown, C.A. Wang, *J. Crystal Growth* 96 (1989) 153.
- [16] C. Park, J.Y. Hwang, M. Huang, T.J. Anderson, *Thin Solid Films* 409 (2002) 88.
- [17] D.W. Kisker, D.R. McKenna, K.F. Jensen, *Mater. Lett.* 6 (1988) 123.
- [18] Z.S. Huang, C. Park, T.J. Anderson, *J. Organomet. Chem.* 449 (1993) 77.
- [19] W. Richter, P. Kurpas, R. Lücknerath, M. Motzkus, *J. Crystal Growth* 107 (1991) 13.
- [20] C. Park, W.-S. Jung, Z. Huang, T.J. Anderson, *J. Mater. Chem.* 12 (2002) 356.
- [21] H.W. Schrötter, H.W. Klöckner, in: A. Weber (Ed.), *Raman Spectroscopy of Gases and Liquids*, Springer, New York, 1979 (Chapter 4).
- [22] J.N. Reddy, *Int. J. Numer. Method Fluids* 2 (1982) 151.
- [23] C.F. Curtiss, R.B. Bird, *Ind. Eng. Chem. Res.* 38 (1999) 2515.
- [24] D.I. Fotiadis, S. Kieda, K.F. Jensen, *J. Crystal Growth* 102 (1990) 441.
- [25] A.H. Dilawari, J. Szekeley, *J. Crystal Growth* 108 (1991) 491.
- [26] N. Suzuki, C. Anayama, K. Masu, *Jpn. J. Appl. Phys.* 25 (1986) 1236.
- [27] M. Suzuki, M. Sato, *J. Electrochem. Soc.: Solid-State Sci. Technol.* 132 (1985) 1684.
- [28] G.H. Evans, R. Greif, *Numer. Heat Transfer* 12 (1987) 243.